View metadata, citation and similar papers at core.ac.uk

brought to you by CORE

provided by Elsevier - Publisher Connector

Biochimica et Biophysica Acta 1818 (2012) 2660–2668

Contents lists available at SciVerse ScienceDirect

Biochimica et Biophysica Acta

journal homepage: www.elsevier.com/locate/bbamem

Membrane adsorption and binding, cellular uptake and cytotoxicity of cell-penetrating peptidomimetics with α-peptide/β-peptoid backbone: Effects of hydrogen bonding and α-chirality in the β-peptoid residues

Xiaona Jing [a], Mingjun Yang [b], Marina R. Kasimova [a], Martin Malmsten [c], Henrik Franzyk [d], Lene Jorgensen [a], Camilla Foged [a], Hanne M. Nielsen [a,*]

[a] Department of Pharmacy, Faculty of Health and Medical Sciences, University of Copenhagen, Universitetsparken 2, DK-2100 Copenhagen, Denmark
[b] Department of Chemistry, Nano-Science Center, University of Copenhagen, Universitetsparken 5, DK-2100 Copenhagen, Denmark
[c] Department of Pharmacy, Uppsala University, Husargatan 3, SE-751 23, Uppsala, Sweden
[d] Department of Drug Design and Pharmacology, Faculty of Health and Medical Sciences, University of Copenhagen, Universitetsparken 2, DK-2100 Copenhagen, Denmark

ARTICLE INFO

Article history:
Received 21 October 2011
Received in revised form 8 April 2012
Accepted 2 May 2012
Available online 16 May 2012

Keywords:
Chirality
Hydrogen bonding
Cell-penetrating peptide
Peptidomimetic
Adsorption
Binding constant

ABSTRACT

Cell-penetrating peptides (CPPs) provide a promising approach for enhancing intracellular delivery of therapeutic biomacromolecules by increasing transport through membrane barriers. Here, proteolytically stable cell-penetrating peptidomimetics with α-peptide/β-peptoid backbone were studied to evaluate the effect of α-chirality in the β-peptoid residues and the presence of guanidinium groups in the α-amino acid residues on membrane interaction. The molecular properties of the peptidomimetics in solution (surface and intramolecular hydrogen bonding, aqueous diffusion rate and molecular size) were studied along with their adsorption to lipid bilayers, cellular uptake, and toxicity. The surface hydrogen bonding ability of the peptidomimetics reflected their adsorbed amounts onto lipid bilayers as well as with their cellular uptake, indicating the importance of hydrogen bonding for their membrane interaction and cellular uptake. Ellipsometry studies further demonstrated that the presence of chiral centers in the β-peptoid residues promotes a higher adsorption to anionic lipid bilayers, whereas circular dichroism results showed that α-chirality influences their overall mean residue ellipticity. The presence of guanidinium groups and α-chiral β-peptoid residues was also found to have a significant positive effect on uptake in living cells. Together, the findings provide an improved understanding on the behavior of cell-penetrating peptidomimetics in the presence of lipid bilayers and live cells.

© 2012 Elsevier B.V. All rights reserved.

1. Introduction

The use of hydrophilic biomacromolecular therapeutics is generally hindered by their poor permeation across the lipid bilayer of the plasma membrane. Consequently, cell-penetrating peptides (CPPs) with a potential to dramatically increase cellular uptake of biomacromolecular drugs have attracted considerable interest during the past two decades. The identification of novel CPP candidates has traditionally involved extensive screening of peptide sequence libraries by studies of cellular uptake and cargo delivery capability. Their cellular uptake mechanism(s) as well as intracellular trafficking have mostly been investigated by the selective inhibition of uptake pathways and tracking of fluorescent cargos [1–5]. However, no consensus has been reached regarding a single unifying mechanism as the preferred route of uptake. Instead it is becoming increasingly evident that uptake pathways vary depending on the properties of both the carrier and the delivered cargo, as well as on the specific biological system studied [6–8].

Irrespective of the internalization mechanism, however, the initial interaction of carrier peptide or peptidomimetic with the membrane is a prerequisite for the subsequent membrane translocation process [9–11]. Previous studies have demonstrated that the guanidinium side chains of arginine, present in many cationic peptidic carriers, play a crucial role for CPP uptake into cells. This is believed to be due to the delocalized cationic charge enabling guanidinium groups transiently to contribute with bidentate hydrogen bonding to cell surface hydrogen bond acceptors [12–14].

Additionally, the effect of chirality on CPP uptake was previously investigated by approaches such as comparison of all-L- and all-D-forms of the same peptide sequence. Uptake was observed for the D-peptide and a retro-inverso analog of penetratin, suggesting that the cellular uptake of CPPs is a chirality-independent process [15,16]. This hypothesis is also supported by more recent studies of polyarginines and Tat peptide analogs [17,18]. Wender et al. reported

* Corresponding author. Tel.: +45 35 33 63 46; fax: +45 35 33 60 01.
E-mail address: hmn@farma.ku.dk (H.M. Nielsen).

0005-2736/$ – see front matter © 2012 Elsevier B.V. All rights reserved.
doi:10.1016/j.bbamem.2012.05.003

that all-D-$Tat_{49–57}$ exhibited an approximately two-fold higher uptake than all-L-$Tat_{49–57}$, and this suggested that the improved cellular uptake is likely due to an increased stability towards proteolysis [13]. The higher uptake efficiency of D-Tat and D-polyarginines was also proposed to be a result of increased proteolytic stability [18,19]. However, it has also recently become evident that the effect of chirality varies among different cell lines. A clear chirality-dependence in the uptake of arginine-containing CPPs (*e.g.* R_9 and penetratin) in MC57 fibrosarcoma and HeLa cells was observed, but not in Jurkat T leukemia cells [20]. To our knowledge, no clear consensus on how chirality influences cellular uptake of CPPs has been reached yet.

In addition to membrane interaction, the proteolytic stability of CPPs is crucial for their *in vitro* and *in vivo* applications, because optimal metabolic stability is required for reaching improved bioavailability of associated cargoes [21–24]. Previously, a series of proteolytically stable guanidinylated α-peptide/β-peptoid chimeras conjugated to carboxyfluorescein (CF) were shown to be taken up by cells four times more efficiently than CF-labeled $Tat_{47–57}$ [25]. The present study provides additional insight into mechanistic details related to the molecular structure of selected peptidomimetics with different structural characteristics. Thus, peptidomimetics based on the α-peptide/β-peptoid hybrid backbone architecture were investigated to elucidate the influence of hydrogen bonding of guanidinium side chains and of α-chirality in the β-peptoid residues on their membrane interaction and cellular uptake. The molecular properties of the peptidomimetics in solution, their structural changes upon interaction with lipid membranes, and the quantification of the adsorbed amounts on anionic lipid bilayers were assessed along with their cellular uptake and cytotoxicity properties.

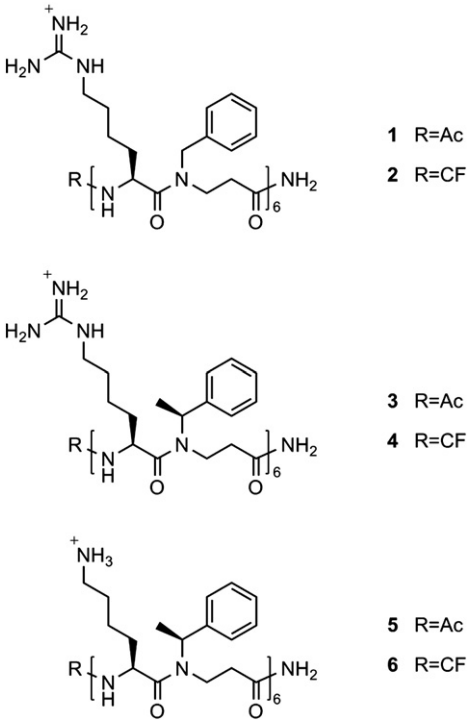

Fig. 1. Chemical structures of the peptidomimetics used in the current study.

2. Materials and methods

2.1. Materials

Amino acids and coupling reagents were obtained from IrisBiotech (Marjtredwitz, Germany). Rink amide resin for the solid-phase synthesis of peptidomimetics was provided by Sigma-Aldrich Chemie (Steinheim, Germany). Ac-$(Arg)_8$-NH_2 (R_8) and N-terminally carboxyfluorescein (CF)-labeled CF-$(Arg)_8$-NH_2 (CF-R_8) were purchased from GenScript (Piscataway, NJ, USA) and were all >98% purity as verified by HPLC and mass spectrometry. Palmitoyl-oleoyl phosphatidylcholine (POPC) and palmitoyl-oleoyl phosphatidylglycerol (sodium salt) (POPG) were both from Avanti Polar Lipids (Alabaster, AL, USA) (>98% purity). HEPES buffer was from AppliChem (Darmstadt, Germany), Hanks Balanced Salt Solution (HBSS) was from Gibco (Paisley, UK), 3-(4,5-dimethylthiazol-2-yl)-5-(3-carboxy-phenyl)-2-(4-sulphophenyl)-2H-tetrazolium (MTS) was from Promega (Madison, WI, USA), and phenazine methosulphate (PMS) was from Sigma (St. Louis, MO, USA). All other chemicals were of analytical grade.

2.2. Synthesis of peptidomimetics

Non-labeled α-peptide/β-peptoid peptidomimetics and CF-labeled compounds (**1**–**6**; Fig. 1) were prepared and characterized as previously reported [26,27].

2.3. Molecular simulation

Four compounds comprising three α-peptide/β-peptoid peptidomimetics (**1**, **3**, and **5**), as well as the control peptide R_8, were selected for molecular simulations. Each compound consists of approximately 200–300 atoms, and the details about simulation model construction and optimization are described below. The compounds were solvated with water to obtain their aqueous structures to mimic conditions similar to the bulk aqueous phase with the *TIP3P* water model. As a result, each molecular system comprises more than 10,000 atoms after adding 3500 explicit water molecules. Briefly, molecular simulation methods can roughly be divided into two categories: quantum mechanics (*QM*) and molecular mechanics or dynamics (*MM*/*MD*) based on an empirical force field. *QM* calculations usually give more accurate results than *MM*/*MD* calculations, but are computationally demanding, especially for relatively large systems like peptide and peptidomimetic structures. On the contrary, *MM*/*MD* calculations using an empirical force field are much faster, but are strongly influenced by the accuracy of the force field. Both *QM* and *MM*/*MD* calculations were used in this study. *QM* calculations were applied to generate force field parameters, which were used in further *MM*/*MD* calculations for long-time simulations of the biomacromolecules in solution. Thus, *QM* calculations were performed using the *Gaussian03* program [28] to develop force field parameters for the studied peptidomimetics. The steps for deriving the force field parameters from the *QM* calculations are as follows: (i) the molecules were built in *Gaussian View*, (ii) the geometry of each of the molecules was optimized, and (iii) the electrostatic potential (*ESP*) derived charges were fitted to reproduce the molecular electrostatic potential, which is a molecular property directly derived from the *QM* self-consist field (*SCF*) calculation. *ESP* charges are known to optimally handle intermolecular properties, which are expected to be critical in our study.

Subsequently, several programs in *Amber version 10* [29–31] were used to generate the peptidomimetic structures. First, the output from *Gaussian* calculations was analyzed with the *antechamber* program to obtain force field parameters. The program *prepgen* was also used to generate all the structure units including either N-terminal or C-terminal end units. Based on these structure units, the peptide and peptidomimetics were constructed with the program *tleap* [30].

After the peptide and peptidomimetics were built, water molecules were added to solvate the molecules with a tool called *Genbox* from *Gromacs*, after which the systems were optimized by energy minimization with *MM* calculations. Further, *MD* calculations were carried out at a temperature of 310 K (37 °C) for 5 ns. The *NVT* (Number, Volume, Temperature) ensemble [32] was used with a time step of 1 fs thus implementing a constant number of particles (N) and

volume (V) at a well-defined temperature (T). This canonical ensemble is a statistical ensemble representing a probability distribution of microscopic states of the system. Based on this, the hydrogen bond number (both surface and intramolecular), the mean square displacement (MSD), as well as the radius of gyration (R_g) were calculated. All the *MM* and *MD* calculations and analyses were performed using *Gromacs 4.5.4* [32]. After 2.5 ns simulation, the total energy and gyration radius for each system became stable, indicating that the system has reached equilibrium. The simulation time of 2.5 ns should be sufficiently long to erase the effect of the starting configurations. *Ewald* summation was used to calculate the electrostatic interactions and the relative strength of the electrostatic interaction at the cutoff of 1.0×10^{-5}.

The number of hydrogen bonds was determined based on cut-off values for the angle of acceptor–donor–hydrogen bonds and the distance between hydrogen–acceptor. The OH and NH groups were regarded as donors, O always as an acceptor, and a hydrogen bond was counted if the length between a donor and an acceptor (bond length) was less than 3.5 Å and the bond angle was smaller than 30°.

The R_g was used to characterize the size of the molecules in solution and was calculated as follows;

$$R_g = \left(\frac{\sum_i^N \|r_i\|^2 m_i}{\sum_i^N m_i}\right)^{\frac{1}{2}} \quad (1)$$

where m_i is the mass of atom i, N is the number of atoms in the molecule, and r_i is the position of atom i with respect to the center of mass of the molecule.

The MSD was used to characterize the dynamic behavior of the molecules as a function of correlation time and was calculated according to Eq. (2).

$$\mathrm{MSD}(\Delta t) = \sum_i^N |r_i(t+\Delta t) - r_i(t)|^2 \quad (2)$$

where $r_i(t)$ is the position of the atom i at time t, N is the number of atoms of a molecule, Δt is the correlation time and the right hand side of the equation represents an average on the time steps.

The slope of the MSD or the so-called diffusion constant (D) can be calculated according to Eq. (3):

$$D = \lim_{\Delta t\to\infty} \frac{1}{6t}\mathrm{MSD}(\Delta t). \quad (3)$$

2.4. Preparation of liposomes

Anionic, unilamellar liposomes (POPC:POPG, 80:20, molar ratio) for the ellipsometry, circular dichroism (CD), and isothermal titration calorimetry (ITC) studies were prepared by the thin film method as described previously [25,33]. Briefly, in order to obtain small unilamellar vesicles (SUVs) for deposition onto supported silica surfaces for the ellipsometry studies, dry lipid films were first formed overnight in round-bottomed flasks under vacuum, after which the lipid films were hydrated in a 10 mM HEPES buffer (pH 7.4) to a final lipid concentration of 6.5 mM. The large multilamellar vesicles (LMVs) formed were subjected to eight freeze–thaw cycles and then extruded 31 times through 30 nm polycarbonate membranes (Whatman, Kent, UK) using a LipoFast Basic extruder (Avestin, Mannheim, Germany). For the CD measurements, the vesicles were extruded 10 times through 50 nm pore size polycarbonate membranes (Whatman, Kent, UK) obtaining a final lipid concentration of approximately 4 mM. For the ITC studies, the lipid films were hydrated for 1 h with vigorous agitation every tenth minute at room temperature with a buffer containing 10 mM HEPES and 150 mM KCl (pH 7.4) to give a lipid concentration of 20 mM. Upon annealing for 1 h, large multilamellar vesicles (LMVs) were extruded (Lipex™ Biomembranes extruder, Vancouver, BC, Canada) 10 times through two stacked polycarbonate membrane filters with 100 nm pore size (Whatman, Herlev, Denmark). For all batches used for ITC, the expected vesicle size and polydispersity index (PDI) were verified by photon correlation spectroscopy. The surface charge of the particles was estimated by analysis of the zeta-potential (Laser-Doppler Electrophoresis). The measurements were performed at 25 °C using a Zetasizer Nano ZS (Malvern, Worcestershire, UK) equipped with a 633 nm laser and 173° detection optics. Malvern DTS v.6.20 software (Malvern, Worcestershire, UK) was used for data acquisition and analysis. For viscosity and refractive index, the values of pure water were used.

2.5. Ellipsometry

The adsorption of the peptides/peptidomimetics to supported lipid bilayers was studied by null ellipsometry using an Optrel Multiskop (Optrel, Kleinmachnow, Germany) equipped with a 100 mW argon laser (532 nm) as described previously [34]. The measurements were carried out at an angle of incidence of 67.52° in a 5 mL cuvette under stirring. The adsorption of lipid as well as peptide and peptidomimetics was monitored by measuring the changes in amplitude and phase of light reflected at the adsorbing surface. The final adsorbed amount (Γ) was calculated using a refractive index increment (dn/dc) of 0.154 cm^3/g [35]. Silica surfaces (Okmetic, Vantaa, Finland) for ellipsometry were prepared from polished silicon slides, which were oxidized to a 30 nm thick oxide layer [36]. Poly-L-lysine (Mw 167.8 kDa, Sigma-Aldrich, Seelze, Germany) was pre-adsorbed to the surfaces prior to lipid deposition to avoid peptide/peptidomimetic adsorption directly onto the silica substrate through any lipid bilayer defects. The supported anionic lipid bilayer was formed by the liposome adsorption method [37] using 30 nm POPC:POPG (80:20 molar ratio) liposomes. After lipid bilayer formation and subsequent rinsing to remove residual liposomes, peptide or peptidomimetic was added to obtain an initial total concentration of 0.01 μM in the cuvette. This initial injection was followed by three subsequent peptide additions to achieve the final concentrations of 0.1, 0.5, and 1 μM. In all cases, the adsorption was monitored for around 1 h or longer until adsorption had stabilized. All measurements were performed at least in duplicates.

2.6. Isothermal titration calorimetry

Thermodynamic analysis of the peptidomimetic adsorption to POPC:POPG liposomes was performed using a Nano ITC (TA Instruments, New Castle, USA) as previously described [33]. Briefly, the reaction cell (V_{cell} = 1 mL), filled with the peptidomimetic dissolved in buffer (10 mM HEPES and 150 mM KCl, pH 7.4), was titrated 10 μL at a time at 5 min intervals into liposome dispersions under constant stirring at 300 rpm at 37 °C. The titrant peptidomimetic concentration was determined spectrophotometrically using an extinction coefficient of 1182 l/mol·cm, and the final concentration in the reaction cell ranged from 19 to 43 μM. For reference purposes, the liposome dispersion was injected into buffer showing constant non-zero heats. Titrations were performed in duplicate and all solutions were degassed prior to use. The data were processed by the software (Nano ITC Run, TA instruments) provided with the Nano-ITC instrument to obtain the injection heats.

2.7. Circular dichroism spectroscopy

The CD spectra of the peptidomimetics in PBS buffer or mixed with a POPC:POPG (80:20 molar ratio) liposome suspension in the same buffer were measured in the range of 200–250 nm with an Olis DSM 10 Spectrophotometer (OLIS, Bogart, GA, USA) using 1 mm quartz cuvettes. The instrument was routinely calibrated for wavelength and optical rotation magnitude with (1S)-(+)-10-Camphorsulfonic acid standard solution (Sigma-Aldrich, St. Louis, MO, USA) using a

two-point calibration. The measurements were performed at 25 °C at a peptidomimetic concentration of 20 μM and a lipid concentration of 2 mM, *i.e.*, at detectable peptidomimetic concentrations and a fixed lipid:peptidomimetic molar ratio of 100:1. All spectra were background-corrected, smoothed, and transformed into mean residue ellipticity [θ]. Data were analyzed using the Globalworks software (OLIS, Bogart, GA, USA) incorporating a digital filtering function [38]. Each spectrum is an average of at least 5 scans.

2.8. Cell culture

HeLa WT cells, Caco-2 cells and Calu-3 cells (ATCC, Manassas, VA, USA) were cultured at 37 °C in an atmosphere of 5% CO_2/95% O_2 in essential medium supplemented with 10% (v/v) fetal bovine serum (FBS) from Fisher Scientific (Hampton, NH, USA), 100 U/mL penicillin and 100 μg/mL streptomycin (both from Sigma-Aldrich, St. Louis, MO, USA). To obtain the complete medium used for culturing the cell lines, Eagle's Minimum Essential Medium (EMEM) used for the HeLa cells was further supplemented with 0.1 mM non-essential amino acids (NEAA, Sigma-Aldrich, St. Louis, MO, USA) and 1 mM sodium pyruvate (Invitrogen, Carlsbad, CA, USA), Dulbecco's Modified Essential Medium (DMEM) used for Caco-2 cells was supplemented with 0.1 mM NEAA and 50 μg/mL gentamicin and for Calu-3 culturing, the DMEM was only further supplemented with 50 μg/mL gentamicin.

2.9. Flow cytometry

HeLa cells (1×10^5 cells per well) were seeded in 24-well tissue culture plates (surface area 1.9 cm^2/well) in 1 mL complete medium (containing 10% (v/v) FBS) and were then incubated for 24 h. The cells were washed with PBS and subsequently incubated with pre-mixed samples containing a total peptide or peptidomimetic concentration of 1 μM or 10 μM in complete medium with FBS for 10 min or 60 min at 37 °C. Afterwards, the cells were washed with PBS and trypsinized, and 1 mL ice-cold PBS containing 10% (v/v) FBS was added to each well. The suspended cells were transferred to tubes, centrifuged (1076×*g*, 4 °C, 5 min) and re-suspended twice, after which the cells resuspended in ice-cold PBS containing 10% (v/v) FBS and 1 μg/mL propidium iodide (PI) (Invitrogen, Carlsbad, CA, USA) were analyzed. The cells were kept on ice prior to analysis. The mean fluorescence was measured with a FACScan flow cytometer (Becton Dickinson, Mountain View, CA, USA) equipped with a 488 nm argon ion laser and 530/30 nm bandpass filter for detection. Dead cells were excluded based on PI staining, and cells exposed to complete medium were used as negative controls (n = 3). Statistically significant differences were assessed by an analysis of variance (ANOVA) at a 0.05 significance level, followed by Tukey's post test.

2.10. Cell viability

The effect of CF-labeled α-peptide/β-peptoid peptidomimetics and CF-R_8 on cellular viability was tested by the MTS/PMS assay, essentially as described previously [39]. Three different cell lines, HeLa, Caco-2 and Calu-3, were cultured in 96-well plates at 37 °C for approximately 24 h in culturing medium until 80–100% confluency. The seeding densities of HeLa, Caco-2 and Calu-3 cells were 9,000, 90,000 and 40,000 cells/well, respectively. The cells were washed with HBSS, and then exposed to solutions of CF-labeled peptidomimetics or CF-R_8 (n = 3) dissolved in complete medium at different concentrations (2 to 256 μM) for 1 h at 37 °C. Immediately after incubation, the cells were washed with HBSS, and 100 μL of freshly prepared MTS/PMS reagent in HBSS was added to each well followed by incubation at 37 °C for 1 h. The dehydrogenase activity was determined by measuring the amount of produced formazan, which has a maximum absorption wavelength of 492 nm. Cells exposed to complete medium were used as negative control, and cells exposed to 0.2% (w/v) SDS as positive control. All values were background-subtracted, and the results are presented as concentration–response curves obtained after data fitting by non-linear regression with four variable parameters as described previously [40].

3. Results

In the present study, three structurally different types of peptidomimetics with membrane-penetrating properties were investigated for membrane interaction using model lipid bilayers as well as live cells, and the obtained results correlated well to molecular simulations of the tested compounds. Both peptidomimetics **1** and **3** had guanidinium groups (Fig. 1), yet construct **3** had α-chiral side chains due to the extra methyl groups in the β-peptoid residues, resulting in a total of six additional chiral centers as compared to construct **1**. Structurally, **3** and **5** differ by the presence of guanidinium groups in **3** and ammonium groups in **5**, respectively.

3.1. Molecular simulations of peptidomimetics in solution revealed four of their molecular properties

The molecular properties of the peptidomimetics and R_8 in solution were calculated from the molecular simulations. Due to the artificial backbone and side chain design of these α-peptide/β-peptoid peptidomimetics, the information available on the structural and dynamical characteristics of this class of molecules is very limited. Currently, there are no conventional methods to measure dihedral angles and determine secondary structures. Since there is no existing parameters available in the literature for *MM*/*MD* calculations of the α-peptide/β-peptoid constructs either, a series of *QM* calculations were utilized to generate a set of force field parameters, which were used in subsequent *MM* and *MD* calculations.

Snapshots of the molecular dynamics of compounds in solution are presented in Fig. 2. The total number of hydrogen bonds between each molecule and solvating water molecules was determined by simulation (Fig. 3A). The order of the peptidomimetics based on decreasing number of hydrogen bonds with water (average in last 2.5 ns) is summarized as **3** (51.6) > **1** (48.8) > **5** (43.9), whereas the number of intramolecular hydrogen bonds (Fig. 3B) resulted in the order **1** (5.64) > **3** (5.30) >> **5** (2.53) (average in last 2.5 ns). The dynamic mobility of the molecules, represented by the slope in Fig. 3C (MSD vs time), decreased in the order of **3** (473 $Å^2$/ns) > **5** (442 $Å^2$/ns) >> **1** (314 $Å^2$/ns). The order of the peptidomimetics based on their decreasing size in water (average R_g) was **3** (8.82 Å) > 5 (8.28 Å) > **1** (7.60 Å) (Fig. 3D). The parameters for the reference peptide R_8 were as follows: average number of hydrogen bonds with water; 49.3; number of intramolecular hydrogen bonds; 0.26; dynamic mobility; 348 $Å^2$/ns, and R_g: 8.73 Å.

3.2. The presence of guanidinium and methyl groups in peptidomimetics results in higher adsorption and binding to anionic lipid bilayers

To further elucidate the influence of different molecular properties of peptidomimetics on their interaction with lipid membranes, the amounts of **1**, **3**, **5** and R_8 adsorbed onto supported anionic lipid bilayers were monitored by ellipsometry. The respective peptidomimetic/peptide concentrations were increased step-wise from 0.01 μM to 1 μM (Fig. 4). The presence of guanidinium groups in **3** resulted in a much higher adsorption than found for its ammonium-substituted counterpart **5** due to the ability of the former to make strong bidentate hydrogen bonds with various anions such as the phosphate head groups of the membrane lipids [41]. When comparing peptidomimetics **1** and **3**, the presence of an extra methyl group introducing α-chirality in the β-peptoid residues in **3** promotes a higher adsorption onto the lipid bilayer.

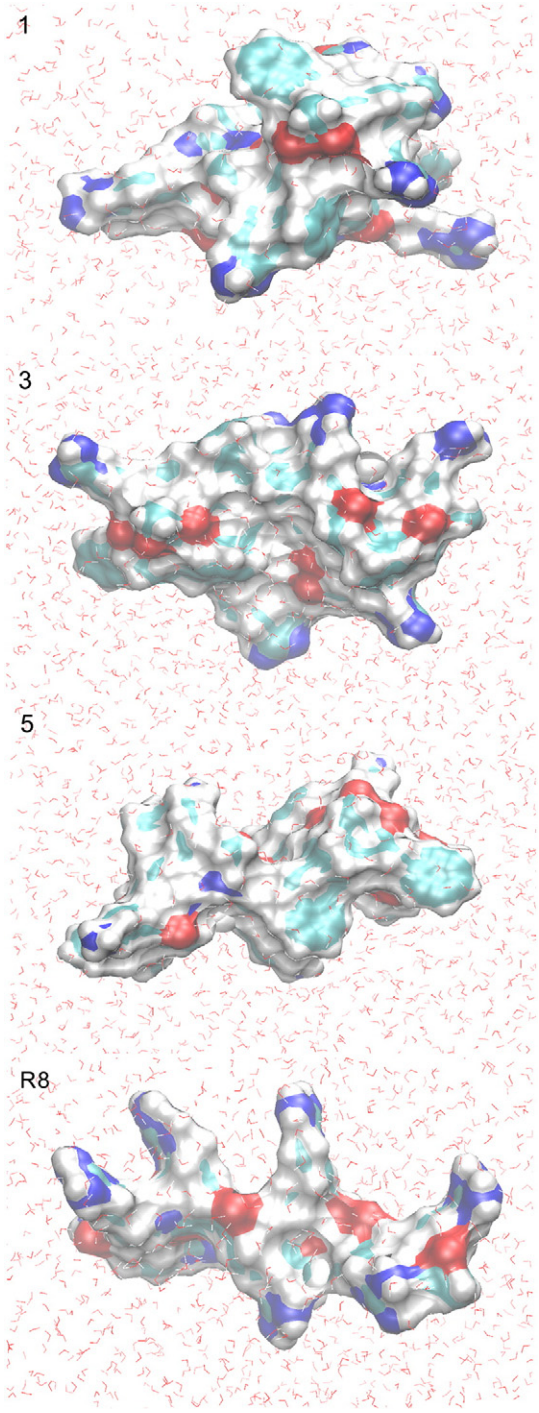

Fig. 2. Snapshots of the molecular dynamics simulations of peptidomimetics **1**, **3** and **5** and peptide R_8 in solution. The snapshots correspond to a probe radius of 1.4 Å. The coloring is depicted according to atom type: blue (nitrogen), red (oxygen), green (carbon) and white (hydrogen).

To obtain quantitative information regarding the thermodynamics of the adsorption process, ITC studies were performed. Data presented in Table 1 show that at physiological temperature the binding enthalpies for **1** and **3** are similar and more favorable than for **5**, yet no significant difference is observed regarding the overall binding energy, ΔG. The values obtained for **1** are comparable with previously reported data [33]. Overall, the bound amount of **5** was significantly less than for the homoarginine-containing peptidomimetics.

3.3. Anionic liposomes influence the folding of partially chiral peptidomimetics to a higher extent as compared to fully chiral peptidomimetics

Complementary to ellipsometry and ITC, CD studies were carried out to elucidate the peptidomimetic structural features in the presence or absence of anionic lipid membranes (Fig. 5).

The comparative circular dichroism studies of the three different peptidomimetics (**1**, **3** and **5**) in buffer clearly showed a higher degree of ordered structure for the fully chiral oligomers **3** and **5**, as compared to the partially chiral oligomer **1** (Fig. 5). Previous studies have shown that α-peptide/β-peptoid oligomers displaying achiral β-peptoid residues exhibit a low degree of ordered structure in the presence of overall neutral DPPC liposomes [42] as well as in an organic medium [26], as compared to the fully chiral analogs, while the minimum of the ellipticity is almost constant (at ~220 nm). Interestingly, comparison of the folding propensity of peptidomimetics **1**, **3** and **5** in the presence of anionic POPC:POPG liposomes in the present study revealed a pronounced shift of the minimum for the mean residue ellipticity observed for partially chiral peptidomimetic **1**, whereas no significant change was seen for the fully chiral **3** and **5** (Fig. 5). Altogether, this suggests that this type of peptidomimetics interacts differently with neutral and anionic liposomes.

3.4. The presence of guanidinium and methyl groups strongly influences cellular uptake, potentially as a result of α-chirality in the β-peptoid residue

To correlate the observations related to the interactions of peptidomimetics with model lipid membranes with their uptake in cells, cellular uptake studies were performed with CF-labeled peptidomimetics using flow cytometry. The overall order of uptake efficiency of the peptidomimetics was conserved at all conditions (Fig. 6). Fully chiral homoarginine-based peptidomimetic **4** showed the highest uptake efficiency in all experiments, while the partially chiral homoarginine-based peptidomimetic **2** ranked second exhibiting comparable uptake within the same order of magnitude, whereas the lysine-based **6** had a significantly lower uptake in the same range as R_8. This is consistent with other studies also demonstrating that arginines present in various CPPs play an important role for their intracellular uptake [43–46]. The effects of incubation time (Fig. 6A and B) and compound concentration (Fig. 6A and C) on the total uptake were also clearly demonstrated. When increasing the peptidomimetic concentration from 1 μM to 10 μM and keeping the incubation time at 60 min, the cellular uptake increased drastically (approximately 30 times for **4**). Similarly, when the incubation time was increased from 10 to 60 min with a fixed concentration of 10 μM, increased cellular uptake was observed for all compounds, but to a lesser extent (approximately 2 times higher for **4**).

3.5. Cell viability

The tolerance threshold of HeLa cells towards exposure to the three CF-labeled peptidomimetics and CF-R_8 (Fig. 7) was investigated for proper assessment of the cellular uptake studies. Overall, concentrations of up to 10 μM of these compounds were well-tolerated in the cells, but at higher concentrations, peptidomimetic **2** and **4** proved more toxic than **6**. The same tendency was observed from studies using proliferating Caco-2 and Calu-3 cells, yet it was evident that the HeLa cells in general were more sensitive to the exposure and that the estimated IC_{50} values varied with the cell line tested.

4. Discussion

The unnatural molecular designs of α-peptide/β-peptoid peptidomimetics were investigated for their membrane interaction and

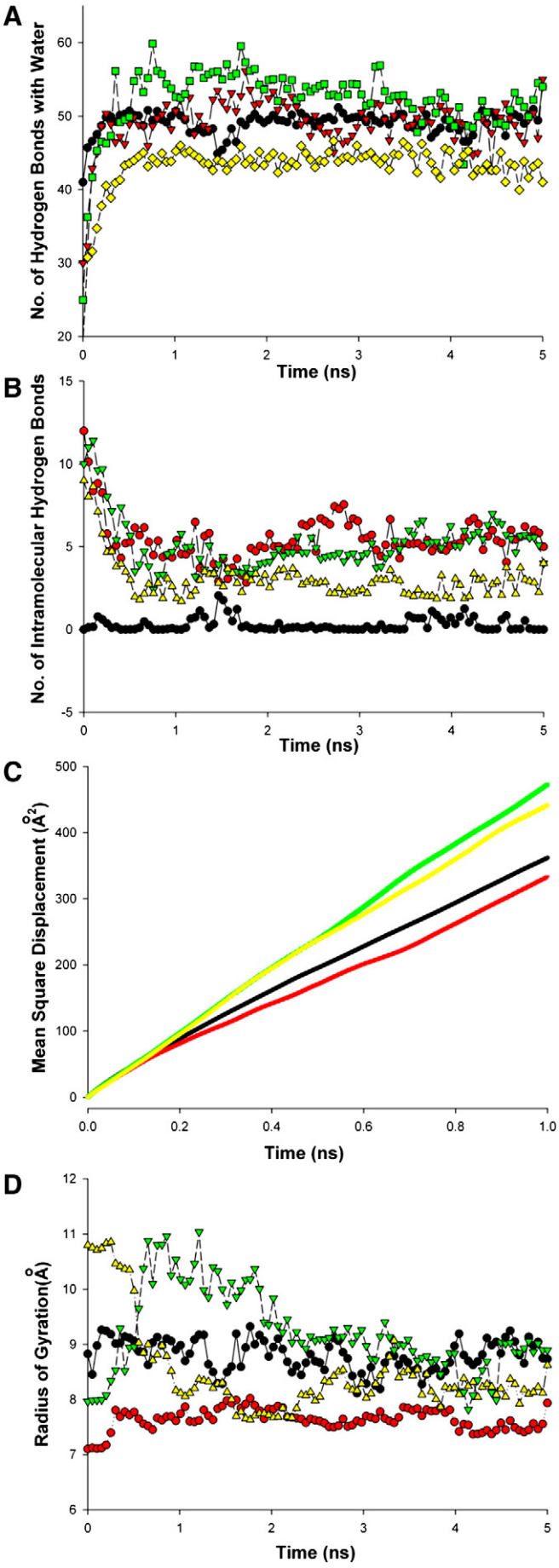

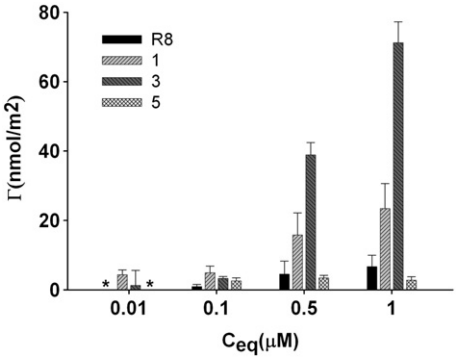

Fig. 4. Adsorption of peptidomimetics (**1**, **3**, and **5**) and R_8 to supported POPC:POPG (80/20) bilayers in HEPES buffer containing 150 mM KCl. * refers to non-detectable adsorption.

cellular uptake as well as toxicity in the current study. Structural characterization of the compounds by NMR has proved fruitless so far because of signal overlap arising from the repetitive nature of the homomeric constructs. Thus, information regarding the secondary structure of these unnatural oligomers is not available, which constitutes a major obstacle to their further molecular understanding. To facilitate correlation and comparison of observed membrane interactions and cellular activities of this recently described class of peptidomimetics, molecular simulation was employed to calculate their molecular properties in solution *e.g.* size, dynamic mobility and intramolecular hydrogen bonding and extramolecular hydrogen bonding with water. When correlating the calculated molecular properties of the peptidomimetics with their membrane adsorption and cellular uptake, it was observed that only the parameter of extramolecular hydrogen bonding with water (Fig. 3A) correlated positively with the observed levels of adsorption to membranes (Fig. 4) and cellular uptake (Fig. 6). This indicates that the number of hydrogen bonding sites on the peptidomimetics might be an important factor for the interaction between the peptidomimetics and lipid membranes as well as for their cellular uptake. Thus, the calculated degree of hydrogen bonding with water reflects the measured adsorption onto lipid membranes, suggesting the latter involves hydrogen bonding with the lipid head groups. In particular, bidentate hydrogen bonds formed between guanidinium-rich peptides and H-bond acceptors on the cell surface have previously been demonstrated to be important for efficient membrane interaction and cellular uptake [41,47]. Furthermore, the ranking of the peptidomimetics based on the intramolecular hydrogen bonding (Fig. 3B) corresponds to the ranking based on their mean residue ellipticity obtained from the CD studies (Fig. 5), suggesting that intramolecular hydrogen bonding capacity might constitute a major structural determinant for folding of the peptidomimetics. On the other hand, the MSD and R_g values obtained from molecular simulations do not seem to be correlated with membrane interaction or cellular uptake, suggesting that these parameters might be functionally less important for membrane interactions and cellular uptake, at least within the parameter range investigated.

The adsorbed amounts of different peptidomimetics onto supported anionic lipid bilayers as measured by ellipsometry showed that the guanidinylated fully chiral peptidomimetic **3** was adsorbed to a substantially higher degree than the corresponding amino-functionalized peptidomimetic **5**. In addition, the adsorbed amount of **3** was higher than the adsorbed amount of the partially chiral

Fig. 3. Time evolutions of (A) the number of hydrogen bonds with water, (B) the number of intramolecular hydrogen bonds, (C) MSD and (D) Rg of three peptidomimetics **1** (red), **3** (green), **5** (yellow) and R_8 (black) from the MD simulations.

Table 1
Thermodynamic parameters for the adsorption of peptidomimetics to POPC:POPG liposomes at 37 °C obtained by fitting the ITC data. The values are presented per mol of peptidomimetic. The experiments were performed in duplicate.

Peptidomimetic	ΔH (kJ/mol)	K (μM^{-1})	n	Bound POPG[a]	ΔG (kJ/mol)	−TΔS (kJ/mol)
1	−22.2	0.19	0.017	6	−31.4	−9.2
	−28.0	0.28	0.013	8	−32.3	−4.3
3	−26.1	0.61	0.017	6	−34.3	−8.3
	−23.9	0.37	0.019	5	−33.1	−9.2
5	−17.9	0.34	0.007	14	−32.9	−14.9
	−17.8	0.46	0.007	14	−33.6	−15.9

[a] Surface POPG per peptide, calculated as 0.1/n, as only 10 mol% of POPG is on the outer surface and thus available for binding.

analog **1**. In the present study, hydrogen bonding, especially when bidentate in nature, between peptidomimetics and lipid membranes, appears to be the predominant interaction force for peptidomimetics **1** and **3**. An overall positive charge is necessary, but not sufficient for efficient adsorption and translocation as seen by the low adsorbed amount and poor cellular uptake of **5** that carries lysine side chains instead of homoarginine side chains. Both the basic lysines (pKa ~10.5), which contains one ammonium group, and the strongly basic homoarginines with a pKa of ~12.5 may be considered fully protonated under physiological conditions, however, the homoarginine residues also possess a delocalized positive charge in the guanidinium group that enables formation of an ion pair [48] or even coordinated bidentate hydrogen bonds [41] with anionic membrane constituents, which promote its adsorption onto and subsequent translocation through membranes. Also, it has been reported that increased hydrophobicity of a protein results in increased adsorption at hydrophobic surfaces [49]. In our study, all peptidomimetics display similar hydrophobic side chains (benzyl or 1-phenylethyl) in the primary sequences. However, the presence of an extra methyl group introducing the side chain α-chirality appears to result in a more favorable arrangement of the hydrophobic residues for membrane adsorption, as peptidomimetic **3** is adsorbed to a higher extent than **1**.

From the ITC experiments, the binding parameters of peptidomimetics **1** and **3** to POPC:POPG membranes are very similar. The CD data indicate that the presence of anionic liposomes induces additional structure in peptidomimetic **1**, but not in peptidomimetic **3**, thus indicating that the existence of secondary structure in the free peptidomimetic has no importance for neither the bound amount nor the enthalpy of binding. The Gibbs free energy of interaction of peptidomimetic **3** was slightly higher than for **1**, although the difference is minor and within the limits of the experimental error. A comparison of the two homoarginine (hArg)-containing peptidomimetics **1** and **3** to the Lys-containing **5** compound shows that this difference in composition is not important for the overall binding energy, ΔG. The enthalpy of interaction is lower for peptidomimetic **5**, suggesting that the heat effect is associated with the presence of guanidinium groups. However, since the overall charge of hArg (pKa ~12.5) and Lys (pKa ~10.5) at pH 7.4 may be considered identical, the difference in ΔH values is not considered to be due to the electrostatic forces. The less favorable enthalpy of interaction of peptidomimetic **5** is compensated by a more favorable entropy, which, according to the CD data, is not caused by structural changes of peptidomimetic **5** upon binding (Fig. 5). Therefore, it is suggested that the more favorable entropy is associated with the effect of peptidomimetic **5** on the lipid bilayer, rather than with the peptidomimetic itself. Indeed, the ellipsometry data indicate that peptidomimetic **5** does not affect the optical properties of the bilayer to the same extent as the other two, thus suggesting that binding of the Lys-containing ligand is more superficial than the interaction of hArg-containing peptidomimetics. In other words, hArg seems to disturb the structure of the lipid bilayer to a higher extent thus

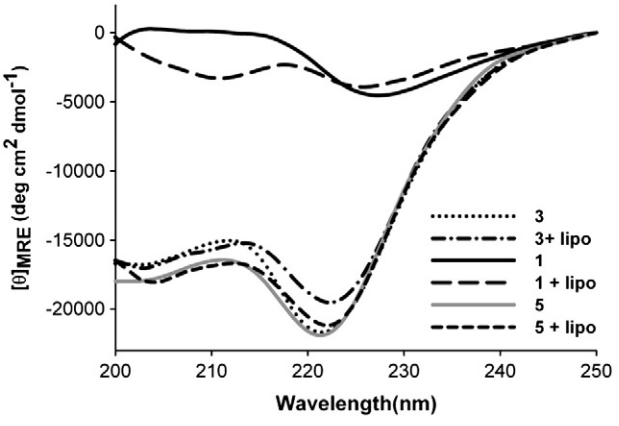

Fig. 5. CD spectra of peptidomimetics in PBS buffer and in the presence of POPC:POPG liposomes (lipo).

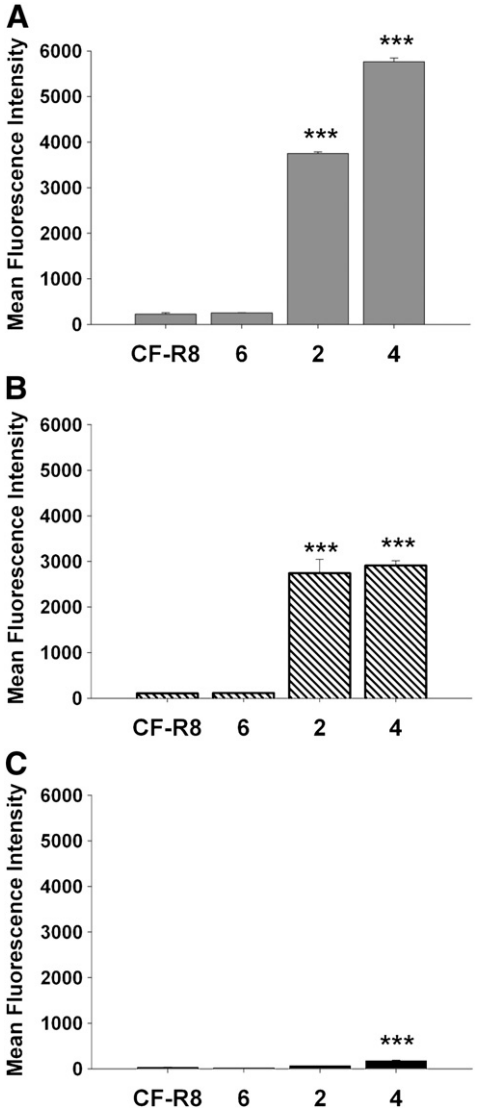

Fig. 6. Cellular uptake of peptidomimetics determined by flow cytometry. HeLa-cells were incubated with CF-labeled peptidomimetic **2**, **4**, **6** or CF-R_8 at 37 °C: (A) at 10 μM for 60 min, (B) at 10 μM for 10 min, and (C) at 1 μM for 60 min. The mean fluorescence intensity data represent mean ± standard deviation of three samples. Significant differences from CF-R_8 are indicated: ***$p<0.001$.

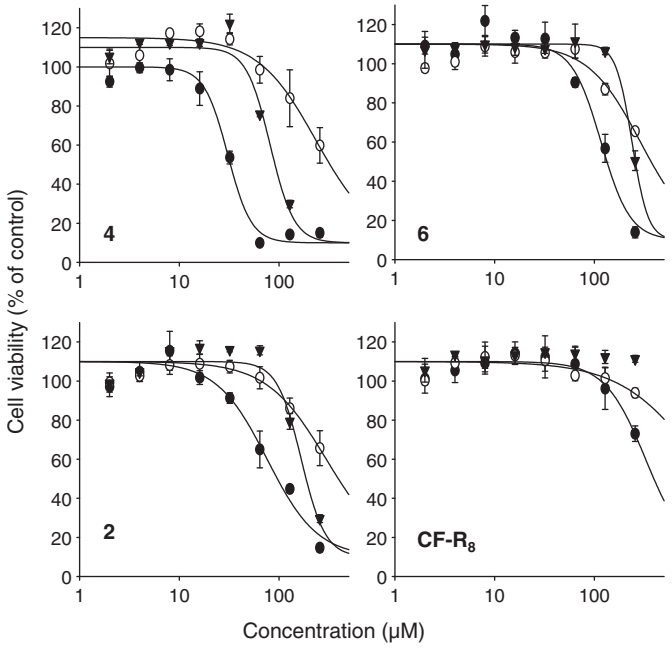

Fig. 7. Effect of CF-labeled peptidomimetics and CF-R_8 on the viability of HeLa (black circle), Caco-2 (black triangle) and Calu-3 cells (white circle). The cell viability after exposure for 1 h was determined by the MTS/PMS assay. The data is expressed as the mean percentage viability relative to the control +/− SD (n = 3).

facilitating a closer interaction between the peptidomimetics and the liposomes. Finally, the bound amount, n, is significantly lower for peptidomimetic **5** than for the other two peptidomimetics, explaining an apparent absence of binding of oligomer **5**, when measured by ellipsometry (Fig. 4). Due to the low n, ellipsometry experiments on this peptidomimetic must be performed at higher concentrations than for oligomers **1** and **3**.

The observation that the CD spectrum of **1** was noticeably altered in the presence of anionic liposomes may be correlated to the absence of the additional methyl branching in the β-peptoid residues of **1**, which obviously results in an increased molecular flexibility of the side chains. By contrast, the bulky methyl group positioned next to the α side chain in **3** and **5** limits the rotational degrees of freedom around the backbone resulting in a more rigid structure.

Uptake experiments with HeLa cells clearly showed the importance of the guanidinium groups, as illustrated by the relatively high uptake of the two homoarginine-rich peptidomimetics **2** and **4** as compared to the lysine-rich peptidomimetic **6** at all concentrations and incubation times tested. The fully chiral **4** was also taken up to a larger extent than the partially chiral counterpart **2**. Overall, the guanidinium-rich, fully chiral peptidomimetic **4** was taken up most efficiently, and its uptake level was significantly higher than that of CF-R_8 under all the tested conditions. These comparative cellular uptake results of peptidomimetics are consistent with the trend found for their adsorption on anionic lipid bilayers by ellipsometry. Moreover, peptidomimetics **2** and **4** exhibited similar cytotoxicity as judged by the cell viability assay, while the ammonium-functionalized **6** was less cytotoxic in all three tested cell lines. At high concentrations, extensive accumulation of the strongly interacting guanidinium-containing peptidomimetics **2** and **4** might eventually lower the cell viability possibly by destabilizing the cell membranes. But overall, the effective concentrations of **2** and **4** are two orders of magnitude lower than the highest concentrations used in the viability assay and none of the concentrations tested in the uptake experiments were shown to be cytotoxic. The ratio of relative uptake efficiency over cytotoxicity indicates the overall benefit of compounds **2** and **4** as compared to **6** and R_8.

5. Conclusions

Molecular simulation of α-peptide/β-peptoid peptidomimetics in solution led to different rankings of the studied compounds based on four molecular properties comprising size, diffusion rate, and hydrogen bonding (both surface and intramolecular). The ranking of the peptidomimetics based on surface hydrogen bonding capacity is in agreement with their efficiency observed in adsorption studies using model membranes and in cellular uptake experiments. Besides the remarkable influence of hydrogen bonding ability of guanidinium groups, the ellipsometry studies also clearly showed that the presence of a methyl group introducing α-chirality of the β-peptoid residues in the peptidomimetics resulted in higher adsorption onto an anionic lipid bilayer. This may be explained not only by the presence of chirality, but also by the additional methyl groups present. However, further structural studies using CD showed that α-chirality influences the overall mean residue ellipticity, and a clear shift of minimum was observed only for the partially chiral compound **1** when interacting with anionic liposomes. The presence of guanidinium groups promoted cellular uptake significantly, but α-chirality of the β-peptoid residues also has a positive influence on the uptake. Increasing the peptidomimetic concentration induced a more pronounced increase in the amount taken up than increasing the incubation time, even at concentrations well tolerated by the HeLa cells. The study demonstrates that thorough molecular understanding, membrane interaction and cellular activity profiling are important for the future design of cell-penetrating peptidomimetics.

Acknowledgements

This work was funded by the Faculty of Pharmaceutical Sciences, University of Copenhagen, Denmark, and the Swedish Research Council. Equipment funding was obtained from The Danish National Advanced Technology Foundation and The Danish Agency for Science, Technology and Innovation. We are grateful to Lise-Britt Wahlberg (Department of Pharmacy, Uppsala University) for excellent technical support. Karina J. Vissing and Maria L. Pedersen (Department of Pharmacy, University of Copenhagen) are acknowledged for assistance with performing the ITC experiments and cell culturing, respectively. We thank Dr. Lovisa Ringstad (Department of Pharmacy, Uppsala University) for scientific advice on ellipsometry, and Mathias Fanø (Department of Pharmacy, University of Copenhagen) for discussion of the CD data. The Danish Center for Scientific Computing (DCSC) is acknowledged for providing the computer resources for molecular simulation.

References

[1] C. Foged, H.M. Nielsen, Cell-penetrating peptides for drug delivery across membrane barriers, Expert Opin. Drug Deliv. 5 (2008) 105–117.
[2] J. Mueller, I. Kretzschmar, R. Volkmer, P. Boisguerin, Comparison of cellular uptake using 22 CPPs in 4 different cell lines, Bioconjug. Chem. 19 (2008) 2363–2374.
[3] M.C. Morris, S. Deshayes, F. Heitz, G. Divita, Cell-penetrating peptides: from molecular mechanisms to therapeutics, Biol. Cell 100 (2008) 201–217.
[4] S.W. Jones, R. Christison, K. Bundell, C.J. Voyce, S.M. Brockbank, P. Newham, M.A. Lindsay, Characterisation of cell-penetrating peptide-mediated peptide delivery, Br. J. Pharmacol. 145 (2005) 1093–1102.
[5] C. Foged, X. Jing, H.M. Nielsen, Cell-penetrating peptides for cytosolic delivery of biomacromolecules, in: V. Weissig, G.G.M. D'Souza (Eds.), Organelle-specific Pharmaceutical Nanotechnology, John Wiley & Sons Ltd, Hoboken, 2010, pp. 403–432.
[6] S.M. Fuchs, R.T. Raines, Pathway for polyarginine entry into mammalian cells, Biochemistry 43 (2004) 2438–2444.
[7] S. Futaki, I. Nakase, A. Tadokoro, T. Takeuchi, A.T. Jones, Arginine-rich peptides and their internalization mechanisms, Biochem. Soc. Trans. 35 (2007) 784–787.
[8] A.T. Jones, Gateways and tools for drug delivery: endocytic pathways and the cellular dynamics of cell penetrating peptides, Int. J. Pharm. 354 (2008) 34–38.
[9] E. Goncalves, E. Kitas, J. Seelig, Binding of oligoarginine to membrane lipids and heparan sulfate: structural and thermodynamic characterization of a cell-penetrating peptide, Biochemistry 44 (2005) 2692–2702.

[10] M. Lundberg, S. Wikstrom, M. Johansson, Cell surface adherence and endocytosis of protein transduction domains, Mol. Ther. 8 (2003) 143–150.
[11] T.B. Potocky, J. Silvius, A.K. Menon, S.H. Gellman, HeLa cell entry by guanidinium-rich β-peptides: importance of specific cation-cell surface interactions, Chembiochem 8 (2007) 917–926.
[12] J.B. Rothbard, D.J. Mitchell, D.T. Kim, L. Steinman, C.G. Fathman, Polyarginine enters cells more efficiently than other polycationic homopolymers, J. Pept. Res. 56 (2000) 318–325.
[13] P.A. Wender, D.J. Mitchell, K. Pattabiraman, E.T. Pelkey, L. Steinman, J.B. Rothbard, The design, synthesis, and evaluation of molecules that enable or enhance cellular uptake: peptoid molecular transporters, Proc. Natl. Acad. Sci. U. S. A. 97 (2000) 13003–13008.
[14] P.A. Wender, W.C. Galliher, E.A. Goun, L.R. Jones, T.H. Pillow, The design of guanidinium-rich transporters and their internalization mechanisms, Adv. Drug Deliv. Rev. 60 (2008) 452–472.
[15] J. Brugidou, C. Legrand, J. Mery, A. Rabie, The retro-inverso form of a homeobox-derived short peptide is rapidly internalized by cultured neurons: a new basis for an efficient intracellular delivery system, Biochem. Biophys. Res. Commun. 214 (1995) 685–693.
[16] D. Derossi, S. Calvet, A. Trembleau, A. Brunissen, G. Chassaing, A. Prochiantz, Cell internalization of the third helix of the antennapedia homeodomain is receptor-independent, J. Biol. Chem. 271 (1996) 18188–18193.
[17] D.J. Mitchell, D.T. Kim, L. Steinman, C.G. Fathman, J.B. Rothbard, Polyarginine enters cells more efficiently than other polycationic homopolymers, J. Pept. Res. 56 (2000) 318–325.
[18] P.A. Wender, D.J. Mitchell, K. Pattabiraman, E.T. Pelkey, L. Steinman, J.B. Rothbard, The design, synthesis, and evaluation of molecules that enable or enhance cellular uptake: peptoid molecular transporters, Proc. Natl. Acad. Sci. 97 (2000) 13003–13008.
[19] G. Tünnemann, G. Ter-Avetisyan, R.M. Martin, M. Stöckl, A. Herrmann, M.C. Cardoso, Live-cell analysis of cell penetration ability and toxicity of oligo-arginines, J. Pept. Sci. 14 (2008) 469–476.
[20] W.P.R. Verdurmen, P.H. Bovee-Geurts, P. Wadhwani, A.S. Ulrich, M. Hallbrink, T.H. van Kuppevelt, R. Brock, Preferential uptake of L- versus D-amino acid cell-penetrating peptides in a cell type-dependent manner, Chem. Biol. 18 (2011) 1000–1010.
[21] A. Amantana, H.M. Moulton, M.L. Cate, M.T. Reddy, T. Whitehead, J.N. Hassinger, D.S. Youngblood, P.L. Iversen, Pharmacokinetics, biodistribution, stability and toxicity of a cell-penetrating peptide-morpholino oligomer conjugate, Bioconjug. Chem. 18 (2007) 1325–1331.
[22] E. Koren, A. Apte, R.R. Sawant, J. Grunwald, V.P. Torchilin, Cell-penetrating TAT peptide in drug delivery systems: proteolytic stability requirements, Drug Deliv. 18 (2011) 377–384.
[23] H.M. Moulton, D.S. Youngblood, S.A. Hatlevig, J.N. Hassinger, P.L. Iversen, Stability of cell-penetrating peptide-morpholino oligomer conjugates in human serum and in cells, Bioconjug. Chem. 18 (2007) 50–60.
[24] C. Palm, M. Jayamanne, M. Kjellander, M. Hallbrink, Peptide degradation is a critical determinant for cell-penetrating peptide uptake, Biochim. Biophys. Acta Biomembr. 1768 (2007) 1769–1776.
[25] C. Foged, H. Franzyk, S. Bahrami, S. Frokjaer, J.W. Jaroszewski, H.M. Nielsen, C.A. Olsen, Cellular uptake and membrane-destabilising properties of α-peptide/β-peptoid chimeras: lessons for the design of new cell-penetrating peptides, Biochim. Biophys. Acta Biomembr. 1778 (2008) 2487–2495.
[26] C.A. Olsen, G. Bonke, L. Vedel, A. Adsersen, M. Witt, H. Franzyk, J.W. Jaroszewski, α-peptide/β-peptoid chimeras, Org. Lett. 9 (2007) 1549–1552.
[27] C.A. Olsen, M. Lambert, M. Witt, H. Franzyk, J.W. Jaroszewski, Solid-phase peptide synthesis and circular dichroism study of chiral beta-peptoid homooligomers, Amino Acids 34 (2008) 465–471.
[28] M.J. Frisch, G.W. Trucks, H.B. Schlegel, G.E. Scuseria, M.A. Robb, J.R. Cheeseman, J.A. Montgomery Jr., T. Vreven, K.N. Kudin, J.C. Burant, J.M. Millam, S.S. Iyengar, J. Tomasi, V. Barone, B. Mennucci, M. Cossi, G. Scalmani, N. Rega, G.A. Petersson, H. Nakatsuji, M. Hada, M. Ehara, K. Toyota, R. Fukuda, J. Hasegawa, M. Ishida, T. Nakajima, Y. Honda, O. Kitao, H. Nakai, M. Klene, X. Li, J.E. Knox, H.P. Hratchian, J.B. Cross, C. Adamo, J. Jaramillo, R. Gomperts, R.E. Stratmann, O. Yazyev, A.J. Austin, R. Cammi, C. Pomelli, J.W. Ochterski, P.Y. Ayala, K. Morokuma, G.A. Voth, P. Salvador, J.J. Dannenberg, V.G. Zakrzewski, S. Dapprich, A.D. Daniels, M.C. Strain, O. Farkas, D.K. Malick, A.D. Rabuck, K. Raghavachari, J.B. Foresman, J.V. Ortiz, Q. Cui, A.G. Baboul, S. Clifford, J. Cioslowski, B.B. Stefanov, G. Liu, A. Liashenko, P. Piskorz, I. Komaromi, R.L. Martin, D.J. Fox, T. Keith, M.A. Al-Laham, C.Y. Peng, A. Nanayakkara, M. Challacombe, P.M.W. Gill, B. Johnson, W. Chen, M.W. Wong, C. Gonzalez, J.A. Pople, Gaussian 03, Gaussian, Inc, Pittsburgh PA, USA, 2003.
[29] D.A. Pearlman, D.A. Case, J.W. Caldwell, W.S. Ross, T.E. Cheatham Iii, S. DeBolt, D. Ferguson, G. Seibel, P. Kollman, AMBER, a package of computer programs for applying molecular mechanics, normal mode analysis, molecular dynamics and free energy calculations to simulate the structural and energetic properties of molecules, Comput. Phys. Commun. 91 (1995) 1–41.
[30] D.A.D. Case, T.A. Darden, T.E. Cheatham III, C.L. Simmerling, J. Wang, R.E. Duke, R. Luo, M. Crowley, R.C. Walker, W. Zhang, K.M. Merz, B. Wang, S. Hayik, A. Roitberg, G. Seabra, I. Kolossváry, K.F. Wong, F. Paesani, J. Vanicek, X. Wu, S.R. Brozell, T. Steinbrecher, H. Gohlke, L. Yang, C. Tan, J. Mongan, V. Hornak, G. Cui, H.D. Mathews, M.G. Seetin, C. Sagui, V. Babin, P.A. Kollman, AMBER10, University of California, San Fransisco, CA, USA, 2008.
[31] D.A. Case, T.E. Cheatham, T. Darden, H. Gohlke, R. Luo, K.M. Merz, A. Onufriev, C. Simmerling, B. Wang, R.J. Woods, The Amber biomolecular simulation programs, J. Comput. Chem. 26 (2005) 1668–1688.
[32] B. Hess, C. Kutzner, D. van der Spoel, E. Lindahl, GROMACS 4: algorithms for highly efficient, load-balanced, and scalable molecular simulation, J. Chem. Theory Comput. 4 (2008) 435–447.
[33] X. Jing, M.R. Kasimova, A.H. Simonsen, L. Jorgensen, M. Malmsten, H. Franzyk, C. Foged, H.M. Nielsen, Interaction of peptidomimetics with bilayer membranes: biophysical characterization and cellular uptake, Langmuir 28 (2012) 5167–5175.
[34] M. Malmsten, Ellipsometry studies of protein adsorption at lipid surfaces, J. Colloid Interface Sci. 168 (1994) 247–254.
[35] M. Malmsten, N. Burns, A. Veide, Electrostatic and hydrophobic effects of oligopeptide insertions on protein adsorption, J. Colloid Interface Sci. 204 (1998) 104–111.
[36] B.E.H. Deal, C.R., The Physics and Chemistry of SiO_2 and the Si–SiO_2 Interface, Plenum Press, New York, 1988.
[37] A. Schmidtchen, M. Pasupuleti, M. Morgelin, M. Davoudi, J. Alenfall, A. Chalupka, M. Malmsten, Boosting antimicrobial peptides by hydrophobic oligopeptide end tags, J. Biol. Chem. 284 (2009) 17584–17594.
[38] P.A. Gorry, General least-squares smoothing and differentiation by the convolution (Savitzky-Golay) method, Anal. Chem. 62 (1990) 570–573.
[39] J. Jacobsen, M. Pedersen, M.R. Rassing, TR146 cells as a model for human buccal epithelium: II. Optimisation and use of a cellular sensitivity MTS/PMS assay, Int. J. Pharm. 141 (1996) 217–225.
[40] H.U. Eirheim, C. Bundgaard, H.M. Nielsen, Evaluation of different toxicity assays applied to proliferating cells and to stratified epithelium in relation to permeability enhancement with glycocholate, Toxicol. In Vitro 18 (2004) 649–657.
[41] J.B. Rothbard, T.C. Jessop, R.S. Lewis, B.A. Murray, P.A. Wender, Role of membrane potential and hydrogen bonding in the mechanism of translocation of guanidinium-rich peptides into cells, J. Am. Chem. Soc. 126 (2004) 9506–9507.
[42] C.A. Olsen, H.L. Ziegler, H.M. Nielsen, N. Frimodt-Møller, J.W. Jaroszewski, H. Franzyk, Antimicrobial, hemolytic, and cytotoxic activities of β-peptoid–peptide hybrid oligomers: improved properties compared to natural AMPs, ChemBioChem 11 (2010) 1356–1360.
[43] S. Brase, T. Schroder, N. Niemeier, S. Afonin, A.S. Ulrich, H.F. Krug, Peptoidic amino- and guanidinium-carrier systems: targeted drug delivery into the cell cytosol or the nucleus, J. Med. Chem. 51 (2008) 376–379.
[44] M. Hong, Y.C. Su, T. Doherty, A.J. Waring, P. Puchala, Roles of arginine and lysine residues in the translocation of a cell-penetrating peptide from (13)C, (31)P, and (19)F solid-state NMR, Biochemistry 48 (2009) 4587–4595.
[45] C.A. Paleos, A. Pantos, I. Tsogas, Guanidinium group: a versatile moiety inducing transport and multicompartmentalization in complementary membranes, Biochim. Biophys. Acta Biomembr. 1778 (2008) 811–823.
[46] P.A. Wender, L.R. Wright, J.B. Rothbard, Guanidinium rich peptide transporters and drug delivery, Curr. Protein Pept. Sci. 4 (2003) 105–124.
[47] J.B. Rothbard, T.C. Jessop, P.A. Wender, Adaptive translocation: the role of hydrogen bonding and membrane potential in the uptake of guanidinium-rich transporters into cells, Adv. Drug Deliv. Rev. 57 (2005) 495–504.
[48] N. Sakai, S. Matile, Anion-mediated transfer of polyarginine across liquid and bilayer membranes, J. Am. Chem. Soc. 125 (2003) 14348–14356.
[49] M. Malmsten, A. Veide, Effects of amino acid composition on protein adsorption, J. Colloid Interface Sci. (1996).